Reprogramming metastatic melanoma cells to assume a neural crest cell-like phenotype in an embryonic microenvironment

Paul M. Kulesa*†, Jennifer C. Kasemeier-Kulesa*, Jessica M. Teddy*, Naira V. Margaryan‡, Elisabeth A. Seftor‡, Richard E. B. Seftor‡, and Mary J. C. Hendrix†‡

*Stowers Institute for Medical Research, 1000 East 50th Street, Kansas City, MO 64110; and ‡Children's Memorial Research Center, Feinberg School of Medicine and Robert H. Lurie Comprehensive Cancer Center of Northwestern University, Chicago, IL 60614

Communicated by Elizabeth D. Hay, Harvard Medical School, Boston, MA, December 13, 2005 (received for review August 15, 2005)

Human metastatic melanoma cells express a dedifferentiated, plastic phenotype, which may serve as a selective advantage, because melanoma cells invade various microenvironments. Over the last three decades, there has been an increased focus on the role of the tumor microenvironment in cancer progression, with the goal of reversing the metastatic phenotype. Here, using an embryonic chick model, we explore the possibility of reverting the metastatic melanoma phenotype to its cell type of origin, the neural-crest-derived melanocyte. GFP-labeled adult human metastatic melanoma cells were transplanted *in ovo* adjacent to host chick premigratory neural crest cells and analyzed 48 and 96 h after egg reincubation. Interestingly, the transplanted melanoma cells do not form tumors. Instead, we find that transplanted melanoma cells invade surrounding chick tissues in a programmed manner, distributing along host neural-crest-cell migratory pathways. The invading melanoma cells display neural-crest-cell-like morphologies and populate host peripheral structures, including the branchial arches, dorsal root and sympathetic ganglia. Analysis of a melanocyte-specific phenotype marker (MART-1) and a neuronal marker (Tuj1) revealed a subpopulation of melanoma cells that invade the chick periphery and express MART-1 and Tuj1. Our results demonstrate the ability of adult human metastatic melanoma cells to respond to chick embryonic environmental cues, a subset of which may undergo a reprogramming of their metastatic phenotype. This model has the potential to provide insights into the regulation of tumor cell plasticity by an embryonic milieu, which may hold significant therapeutic promise.

plasticity | chick | MART-1 | epigenetic

Cancer is a complex disease involving a dynamic relationship between tumor cells and their microenvironment. Particularly challenging is the issue of tumor cell plasticity, which shares many properties in common with embryonic cells, including a dedifferentiated phenotype. Following this general theme, Mintz and Illmensee (1) addressed the basic question of whether the embryonic microenvironment of a mouse blastocyst could possibly revert the metastatic phenotype of teratocarcinoma cells. Surprisingly, the tumorigenic phenotype of the teratocarcinoma cells was suppressed by the mouse embryonic microenvironment, whereas the developmental plasticity of the tumor cells was manifested as the tumor cells contributed to the formation of normal tissues. With a chick embryo model, a similar tumor-suppressing microenvironment was observed when Rous sarcoma virus (RSV) induced sarcomas in chick hatchlings but failed to do so in embryos (2). When sarcoma 180 cells were transplanted into the chicken embryo, cells loosely spread into the tissue as single cells forming some occasional clumps (3). Indeed, attempts to revert or reprogram the metastatic phenotype of tumor cells by microenvironmental cues has been an area of intense study that has benefited from technological advances and experimental approaches (4), especially evident in a recent, exciting study by Jaenisch and colleagues (5), who transferred the nuclei of various malignant melanoma mouse cells into enucleated oocytes and derived ES cells from the cloned mouse embryos. The resulting cloned ES cells were pluripotent and generated normal-appearing chimeric mice, further demonstrating that the cancer phenotype of the donor cells is reversible.

In an effort to dissect the tumor cell microenvironment interactions, using melanoma as a model, we analyzed the molecular profile of highly aggressive vs. poorly aggressive melanoma cells (6). These studies revealed that highly aggressive human metastatic melanoma cells have a molecular signature characteristic of a plastic, dedifferentiated cell type (7). Furthermore, metastatic melanoma cells down-regulate melanocyte-specific markers, consistent with a dedifferentiated phenotype (6–8). To further our understanding of the biological relevance of melanoma plasticity, we studied the fate of melanoma cells in two experimental models: (*i*) an ischemic limb model and (*ii*) a zebrafish embryo. In the first model, fluorescently labeled metastatic melanoma cells were challenged to an ischemic microenvironment surgically induced in the hind limbs of nude mice (9). This study demonstrated the capability of these tumor cells to express embryonic cell fate-determination molecules and to participate in neovascularization of the limb by forming chimeric blood vessels with mouse endothelial cells. In the second model, GFP-labeled metastatic melanoma cells were transplanted (and followed up to 3 months posttransplantation) into zebrafish blastula-stage embryos, which resulted in the loss of their tumorigenic properties (10). Both of these studies underscore the remarkable developmental plasticity of mesenchymal-lineage melanoma cells and beg the question of which embryonic signaling mechanism(s) might be responsible for reverting the metastatic phenotype. Indeed, the application of developmental-biology principles to the study of cancer biology will yield new perspectives on tumor cell plasticity (11).

In the developing vertebrate embryo, the normal patterning of peripheral structures and the nervous system involves the invasion of a multipotent population of cells known as the neural crest. Neural crest cells (NCCs) arise along the vertebrate axis in the dorsal neural tube and migrate into the surrounding tissue to give rise to bone and cartilage, neurons and glia of the peripheral nervous system, and pigment cells (12). NCCs follow stereotypical migratory pathways, forming segregated streams of cells that emerge adjacent to specific locations along the vertebrate axis (13–16). Although NCCs arise along the dorsal neural tube, NCCs avoid migrating into certain areas adjacent to the neural tube, such that NCC-free zones arise between migratory streams (17–20). When NCCs invade these areas, cells either stop and collapse filopodia or alter their trajectories to join a neighboring stream (16),

Conflict of interest statement: No conflicts declared.

Abbreviations: ba, branchial arch; DRG, dorsal root ganglia; NCC, neural crest cell; r rhombomere; SG, sympathetic ganglia.

†To whom correspondence may be addressed. E-mail: mjchendrix@childrensmemorial.org or pmk@stowers-institute.org.

www.pnas.org/cgi/doi/10.1073/pnas.0506977103

suggesting the presence of a local environmental inhibitory signal(s). Intensive investigations using tissue transplantations, cell labeling, and molecular analyses suggest that the NCC migratory streams are sculpted from a combination of intrinsic and local extrinsic cues in the microenvironment (21–24).

Collectively, our observations of the plastic phenotype of melanoma cells and our experimental model of NCCs led us to hypothesize that metastatic melanoma cells could respond to an embryonic microenvironment experienced by their ancestral cell type, the NCC. In this study, we transplanted GFP-labeled human metastatic melanoma cells into the embryonic chick neural tube and showed that these tumor cells invade the chick periphery in a programmed manner along stereotypical NCC migratory pathways and populate peripheral destinations. A subpopulation of the invading melanoma cells express melanocyte and neuronal markers previously undetected at the time of transplantation. Taken together, our results suggest that human metastatic melanoma cells respond to and are influenced by the chick embryonic neural-crest-rich microenvironment, which may hold significant promise for new therapeutic strategies.

Results

Melanoma Cells Invade Chick Embryo Tissues in a Programmed Manner. To determine whether metastatic melanoma cells invade embryonic chick tissues in a programmed or indiscriminate manner, we transplanted adult, GFP-labeled human metastatic melanoma cells into the rostral neural tube of young, 7- to 9-somite chick embryos. At these stages, the host NCCs are either just beginning to emerge or have not yet emerged from the neural tube. Before the transplantation of the melanoma cells, we injected the fluorescent, lipophilic carbocyanine dye DiI into the neural tube to label host chick NCCs. After 48 h of egg reincubation, the positions of the transplanted melanoma cells were analyzed. At this time, we found that melanoma cells invade the mesoderm lateral to the chick neural tube when transplanted into regions of the rostral neural tube from which NCC streams typically emerge (Fig. 1). Invading metastatic melanoma cells do not form tumors, even after extended egg reincubation up to 96 h (see Fig. 6 *H–J*, which is published as supporting information on the PNAS web site) but distribute as individual cells with a salt-and-pepper-like distribution along stereotypical cranial NCC migratory pathways (Fig. 1). However, the GFP-labeled metastatic melanoma cells form primary tumors within 1 week in nude mice and, subsequently, metastasize to the lung, as shown in Fig. 6 (*K* and *L*). When these melanoma cells are transplanted near the midbrain, the tumor cells disperse into the mesoderm to populate distal portions of the head (Fig. 1 *A–C*). Metastatic melanoma cells transplanted into rhombomere (r)2 resulted in the tumor cells populating the distal 1st branchial arch (ba)1 and joining host NCCs (Fig. 1 *D–F*). When melanoma cells were transplanted into r6, the cells reached the ba4 (Fig. 1 *G–I*). Time-lapse imaging sessions confirmed that transplanted metastatic melanoma cells invade the chick tissue and follow NCC migratory pathways (Fig. 6 *S* and *T*; and see Movies 1 and 2, which are published as supporting information on the PNAS web site). C81-61 poorly aggressive melanoma cells, the isogenic counterpart of the metastatic C8161 tumor cells, transplanted into similar regions in chick hosts did not invade the surrounding tissue (Fig. 6 *D–G*).

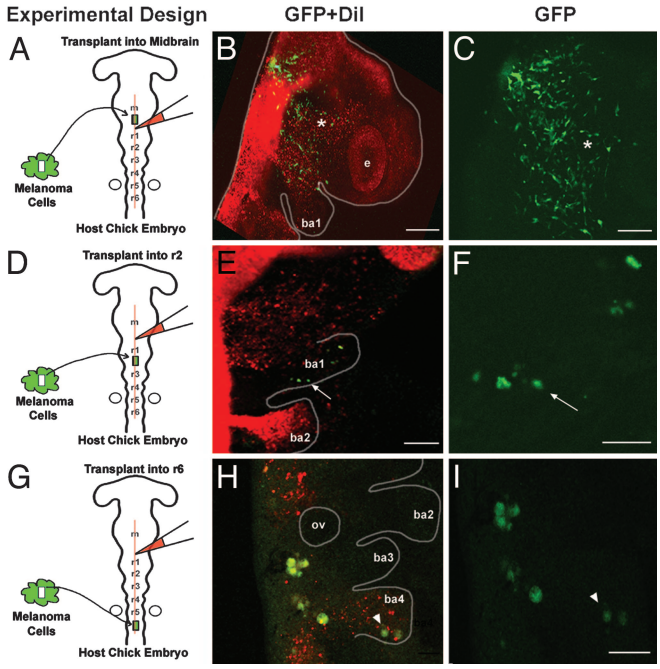

Fig. 1. Transplanted metastatic melanoma cells invade chick cranial NCC migratory pathways and destinations. Chick embryos (6- to 8-somite stage) were injected with a lipophilic dye, DiI, into the rostral neural tube to label premigratory NCCs. Adult human metastatic melanoma cells (C8161) were then transplanted into specific cranial neural tube locations in the host chick embryos, one small block of melanoma cells per host chick embryo. Eggs were resealed and reincubated for 48 h. (*A–C*) GFP-labeled melanoma cells, transplanted as a small clump of cells into the chick midbrain (m) region invade host tissue and spread out toward the ba1 and eye (e). (*B* and *C*) The GFP-labeled melanoma cells (green) migrate with the host chick NCCs (red; asterisk) along the stereotypical NCC pathway. (*D–F*) GFP-labeled melanoma cells (green) transplanted into r2 spread out to populate ba1 (arrow), together with host chick NCCs (red). (*G–I*) GFP-labeled melanoma cells (green; arrowhead) transplanted into r6 reach the ba4 with host chick NCCs (red). A total of 128 transplantations were performed, one transplant per embryo. The otic vesicle (ov) is labeled. [Scale bars, 100 μm (*B* and *C*) and 50 μm (*E*, *F*, *H*, and *I*).]

Invading Melanoma Cell Morphologies Resemble Host NCCs. High-resolution confocal imaging reveals that invading adult human metastatic melanoma cells display cell morphologies that resemble chick NCCs (Fig. 2). In a typical host chick embryo, many transplanted melanoma cells demonstrate a bipolar shape (Fig. 2 *A* and *B*). Melanoma cell filopodia are typically long (≈50 μm) and thin (≈1–5 μm). When compared with host NCCs, melanoma cell filopodia are approximately similar in size (Fig. 2 *A* and *B*). Transplanted melanoma cells also display thin filopodial connections between neighboring cells (Fig. 2 *C* and *D*). The lengths of the connections are similar in size to those observed between host NCCs (Fig. 2 *C* and *D*). Surprisingly, transplanted melanoma cells also form linear chain-like arrays, similar to the collective migratory feature of host NCCs (Fig. 2 *E* and *F*). However, the lengths of the melanoma-cell chain-like arrays are longer than NCC chains (Fig. 2 *E* and *F*). The directionality of the melanoma cells coincides with the direction toward the branchial arches. We performed cell counts to determine the distribution and location of NCCs and metastatic melanoma cell morphologies (Fig. 2 *G* and *H*). In contrast to the NCCs, transplanted metastatic melanoma cells had less hairy cell morphologies midstream (25% vs. 65%) but more bipolar-shaped morphologies (55% vs. 18%) (Fig. 2 *G* and *H*). In the branchial arches, the metastatic melanoma cells had more bipolar-shaped morphologies (13% vs. 5%) and less hairy shapes (7% vs. 12%) than the NCCs (Fig. 2 *G* and *H*).

Melanoma Cells Transplanted into the Trunk Neural Tube Maintain Segregated Streams and Populate Dorsal Root Ganglia (DRG) and Sympathetic Ganglia (SG) Sites. To examine whether metastatic melanoma cells invade and populate trunk structures, we transplanted the GFP-labeled tumor cells into the caudal neural tube of chick embryos (Fig. 3 *A* and *B*). In a typical chick embryo, the first emerging trunk NCCs migrate along the dorsoventral pathway and through the rostral somite and arrest dorsally near the neural tube to form the DRG or continue eventually toward the dorsal aorta to

MEDICAL SCIENCES

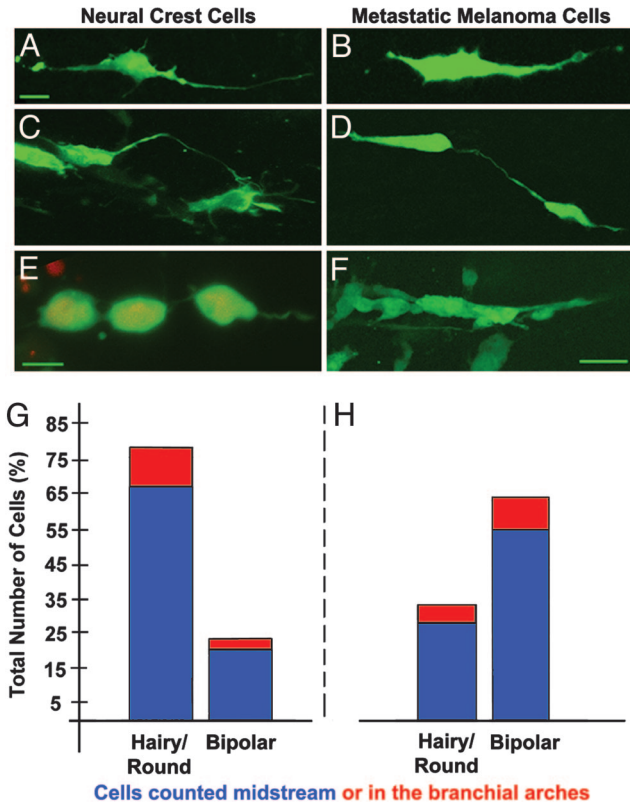

Fig. 2. Transplanted metastatic melanoma cells and chick NCCs share *in vivo* cell morphologies along host NCC migratory pathways. The images demonstrate three commonly observed cell morphologies of host chick NCCs and human melanoma cells transplanted into chick embryos. (*A* and *B*) The first example shows typical host chick NCCs (*A*) and transplanted melanoma cells (*B*) displaying long filopodial extensions. Both cell types display a bipolar phenotype. (*C* and *D*) The second example shows two individual NCCs (*C*) and melanoma cells (*D*) connected by a thin (1–2 μm) filopodial connection. (*E* and *F*) The third example shows host chick NCCs (*E*) and melanoma cells (*F*) displaying collective cell migratory structures in linear chain-like arrays, with the melanoma cell chains typically longer than the NCCs chains. The NCCs (*A*, *C*, and *E*) are labeled with a fluorescent protein construct Gap43-EGFP and double-labeled in *E* with H2B-mRFP. [Scale bars, 10 μm (*A–E*) and 50 μm (*F*).] (*G* and *H*) The graphs represent the number of hairy/round vs. bipolar-shaped cells counted after analyzing migrating neural crest (*G*) and metastatic melanoma (*H*) cells invading the chick embryo. (*G*) In a typical fluorescently labeled chick embryo (n = 9 embryos; n = 361 NCCs counted), the blue bars represent NCCs in the middle of NCC migratory streams vs. in the branchial arches (red).

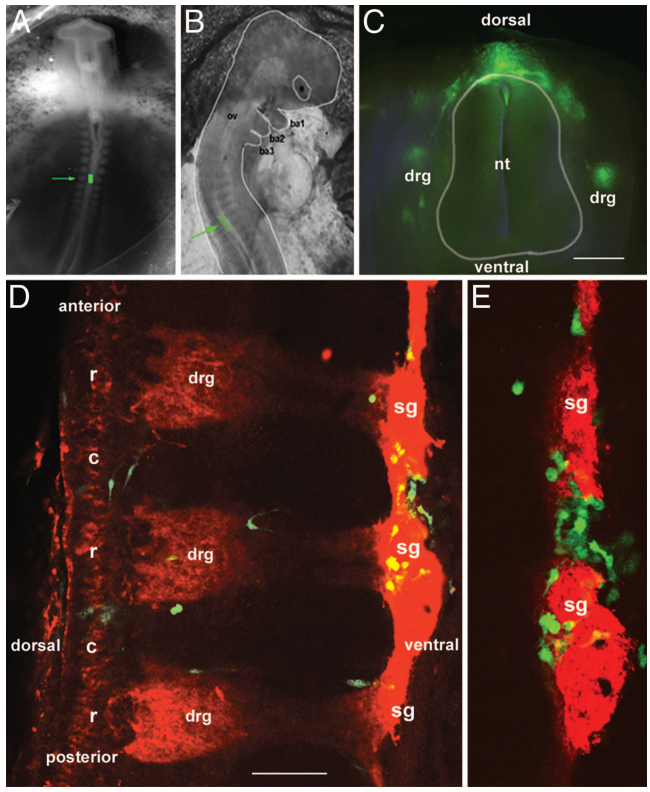

Fig. 3. Metastatic melanoma cells transplanted into the chick trunk neural tube invade DRG and SG sites. (*A*) Metastatic melanoma cells are transplanted into the trunk neural tube (arrow) in a typical chick embryo host with 9–11 somites and (*B*) incubated for ≈48 h. The location of the melanoma cell transplant is shown by the green square and arrow in a typical embryo. (*C*) A transverse view through the trunk region of a typical chick embryo in the region of the transplanted melanoma cells (green) 48 h after transplantation and incubation (the outline surrounds the neural tube). A thick transverse section was cut through the embryo (200 μm) by using a razor blade and laid flat to reveal ventral tissues. The melanoma cells (green) have migrated from the dorsal neural tube to the DRG and further ventral. Melanoma cells also appear along a dorsolateral route. (*D*) A sagittal view through a typical chick embryo in the region of the transplanted melanoma cells (green) 48 h after transplantation. The embryo was cut in half down the anterior–posterior axis and laid flat to reveal ventral tissues. The background staining is HNK-1 (red), showing the host chick trunk NCCs migrating in stripes through the rostral, but not the caudal, portions of somites. The melanoma cells (green) appear to colocalize with the HNK-1-positive (red) stripes and migrate to the DRG and SG (*E*) The melanoma cells (green) target the forming SG and colocalize with the HNK-1-labeled trunk NCCs (red). A total of 40 transplantations were performed, one transplant per embryo. (Scale bars, 50 μm.)

form the SG. Later-emerging trunk NCCs follow a dorsolateral pathway and give rise to melanocytes. In the host chick embryos that received melanoma cells in the trunk neural tube, the tumor cells migrate preferentially through the rostral somite, colocalizing to the same migratory routes of the trunk NCCs (Fig. 3*C*). Strikingly, very few melanoma cells enter the caudal somite (Fig. 3*D*), a region that NCCs typically avoid. Surprisingly, many melanoma cells migrate ventrally beyond the site of the DRG and stop at the location of SG formation (Fig. 3 *D* and *E*). The melanoma cells disperse in the anterior–posterior direction, mimicking a pattern displayed by host NCCs (Fig. 3*E*). Along the NCC migratory routes, melanoma cells display bidirectional cell morphologies with cellular extensions in the direction toward the lateral periphery (Fig. 3*D*).

Melanoma Cells Reach Host NCC Destinations Independent of a Host NCC Scaffold. To test whether transplanted melanoma cells use host NCCs as a scaffold to reach the periphery, we ablated subpopulations of premigratory host NCCs and replaced them with human metastatic melanoma cells (Fig. 4). We confirmed the loss of the majority of host NCCs after ablations by fluorescently labeling host premigratory NCCs with a lipophilic dye (DiI), injected into the neural tube before ablation. In these embryos, GFP-labeled metastatic melanoma cells continued to invade the host NCC migratory pathways (Fig. 6 *A–D*).

In a typical chick embryo, NCCs from r3, r4, and r5 emerge to form a migratory stream extending lateral to r4, called the r4 stream (Fig. 4 *A–C*). The shape of the chick r4 migratory stream has a wide front (8–9 cells) that tapers (5–6 cells) back to the neural tube and is densely packed (Fig. 4 *A–C*). We focused on the r4 migratory stream because it is easily accessible to manipulation and is visually distinguishable, adjacent to two NCC-free zones. Melanoma cells emerge and populate the peripheral branchial arches in host chick embryos where the premigratory NCCs from mid-r3 to mid-r5 are ablated (Fig. 4 *D–F*). The melanoma cells form dense migratory streams near the neural tube, similar to a typical chick NCC

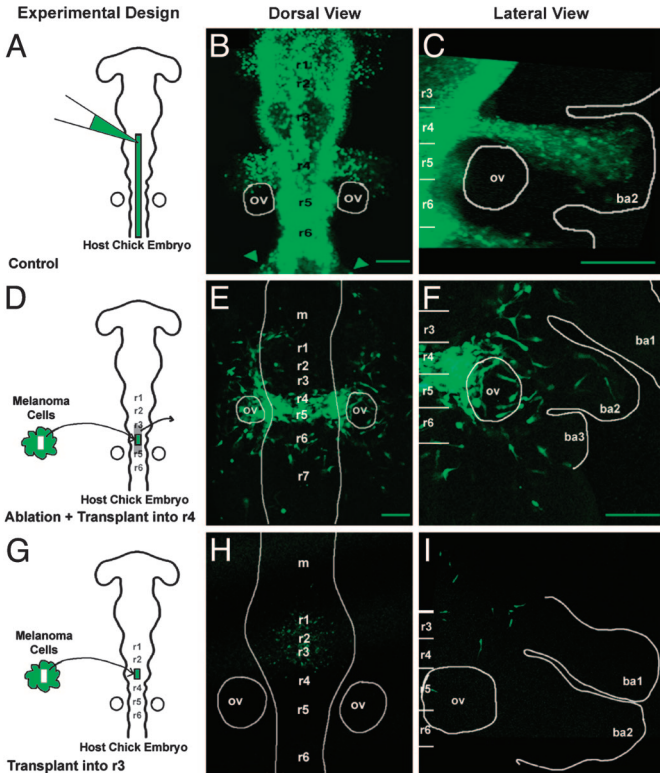

Fig. 4. Transplantation of metastatic melanoma cells into odd-numbered chick rhombomeres after ablation of host chick premigratory NCCs. In normal chick embryos, DiI-labeled cranial NCCs (*A–C*) are sculpted into three stereotypical migratory streams that extend from the rhombomeres (r), r1 and r2, r4, and r6. (*B* and *C*) After 36 h, the streams lead to the branchial arch destinations: NCCs from r3, r4, and r5 form into the r4 migratory stream (*C*) that targets the ba2. (*D–F*) Host mid-r3 to mid-r5 premigratory NCCs are ablated in 9-somite chick embryos after a time when host chick NCCs regenerate. (*E*) Melanoma cells transplanted into r4 form a dense migratory stream along the stereotypical NCC migratory pathway and (*F*) populate the ba2 and ba3 and the region near ba1 when viewed after 48 h. (*G–I*) At 48 h after melanoma cells are transplanted into r3, they do not form into a dense migratory stream to invade the host chick tissue (*H*) but remain fairly confined to the neural tube. (*I*) Only a small number of melanoma cells emerge from the neural tube. A total of 72 ablations plus transplantations were performed, one transplant per embryo. [Scale bars, 100 μm (*B*, *C*, *E*, and *F*); and the scale bars in *E* and *F* can be used for *H* and *I*, respectively.]

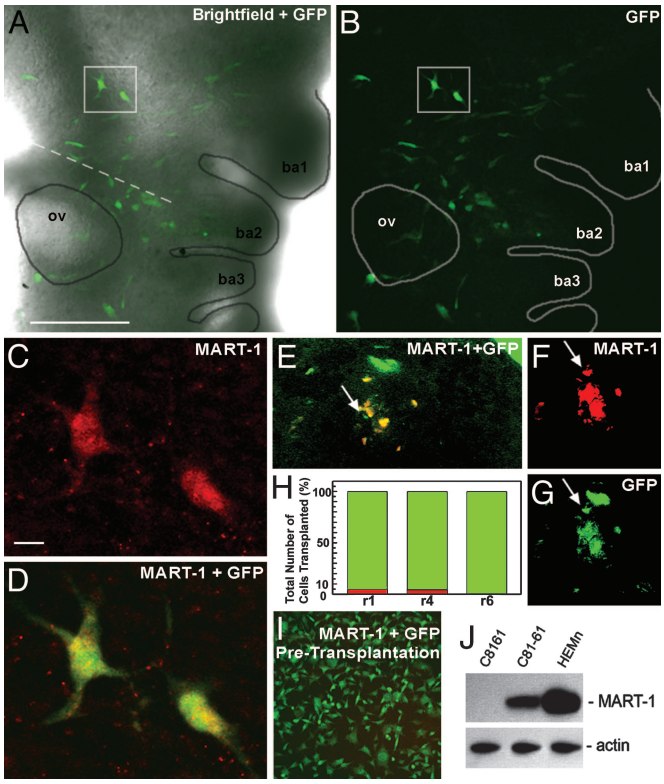

Fig. 5. MART-1 expression of transplanted melanoma cells after invading host chick embryonic tissues. (*A*) A typical chick embryo 48 h after transplantation of GFP-labeled (green) metastatic melanoma cells and reincubation. (*A* and *B*) The GFP-labeled melanoma cells (green) invade the chick host periphery around the otic vesicle (ov, circled) and target the ba1–ba3 (outlined). (*A–D*) After fixation and staining for MART-1, the box surrounds two individual melanoma cells that are shown magnified in *C* and *D* positive for MART-1 expression. (*E–H*) Further analysis of invading melanoma cells in tissue sections shows that a number of melanoma cells express MART-1. The location of a typical tissue section is shown by a dotted line in *A*. (*H*) The bar graph plots the percent number of MART-1-positive melanoma cells (red) vs. the total number of GFP-labeled metastatic melanoma cells (green) transplanted into r1, r4, and r6. (*I*) Before transplantation of melanoma cells (C8161) into the chick embryo, melanoma cells were stained for MART-1. (*J*) Western blot analysis for the expression of MART-1 in cell lysates of the human melanoma cell lines C8161 (highly aggressive and metastatic) and C81-61 (poorly aggressive) as well as the human melanocyte cell line HEMn. Fifteen micrograms of protein were loaded per lane of each sample, and Western analysis revealed the presence of MART-1 in C81-61 cells and HEMn melanocytes. An equal loading of the samples is demonstrated by probing the same blot for actin. [Scale bars, 200 μm (*A* and *B*), 15 μm (*C* and *D*).]

migratory stream (Fig. 4 *D–F*). The migratory streams persist to the chick otic vesicle, and then the melanoma cells disassemble and distribute into the peripheral ba1 (Fig. 4*F*). Some melanoma cells migrate to other distal locations, including near the ba1 and ba3 (Fig. 4 *D–F*).

Melanoma Cells Do Not Invade Host NCC-Free Zones. In a typical chick embryo, NCCs that emerge from r3 and r5 avoid the regions lateral to their respective rhombomeres. R3 and r5 NCCs travel along diagonal trajectories to join neighboring cell migratory streams. NCCs that wander into the areas lateral to r3 and r5 either stop or dramatically alter their trajectories toward neighboring streams, suggesting the presence of local inhibitory signals. This migration pattern gives rise to NCC-free zones lateral to r3 and r5. A similar pattern is observed in the trunk, at each axial level of an individual somite. We asked whether human metastatic melanoma cells respond to chick embryonic cues thought to establish and maintain the chick NCC-free zones. When we transplanted melanoma cells into r3, very few tumor cells migrated lateral to r3 (Fig. 4 *G–I*). Transplanted melanoma cells appear to spread out in the anterior-posterior direction along the dorsal neural tube (Fig. 4). However, individual melanoma cells do not invade the ba1 and ba2 as extensively as when transplanted into r1 or r4 (Fig. 4).

A Subpopulation of Transplanted Invading Melanoma Cells Express a Melanocyte Marker (MART-1) and Neural Marker (TuJ1). To test whether transplanted human metastatic melanoma cells express phenotype-specific genes associated with the acquisition of a neural crest melanocyte-like phenotype, we examined chick embryos stained with MART-1, a melanocyte differentiation antigen, expressed on both melanocytes and differentiated melanoma cells that are poorly or moderately aggressive (25). However, the metastatic (amelanotic) tumor cells used in this study have been shown to be negative for MART-1 (7). We find that a subset of transplanted GFP-labeled melanoma cells that invade the chick periphery (Fig. 5 *A* and *B*) are MART-1-positive (Fig. 5 *C* and *D*). Individual tissue sections of the chick embryo (Fig. 5*A*, dotted line) confirm that a number of transplanted GFP-labeled melanoma

MEDICAL SCIENCES

cells express MART-1 (Fig. 5 *E–G*). The number of MART-1-positive melanoma cells is ≈5% and ≈34% of the total number of transplanted melanoma cells into r1 and r4, respectively (Fig. 5*H*). Before transplantation, the GFP-labeled melanoma cells do not express MART-1 by immunofluorescence microscopy (Fig. 5*I*). In addition, Western blot analysis for the expression of MART-1 in cell lysates of the human melanoma cell lines C8161 and C81-61, as well as the human melanocyte cell line HEMn, confirm that the metastatic tumor cells used in this study (C8161) are negative for MART-1 (Fig. 5*J*), whereas their isogenic, poorly aggressive counterpart C81-61 and normal melanocytes HEMn are positive. We also tested whether invading melanoma cells express neuronal (TuJ1 and Hu RNA-binding protein) and glial (P0) markers. A small number (≈13%) of the total number of invading metastatic melanoma cells expressed TuJ1 (Fig. 6 *M–R*). Collectively, these data indicate a possible reversion of a subset of transplanted human metastatic melanoma cells to neural-crest-derived melanocyte-like and neuronal-like phenotype(s) because of their interactions with the chick embryonic NCC microenvironment.

Discussion

The ultimate goal of our work is to decipher the molecular signals within a microenvironment that inhibit destructive tumor cell properties and/or cause a reversion to a nonaggressive phenotype. In this study, we transplanted GFP-labeled adult human metastatic melanoma cells into the chick-embryo microenvironment and assayed the details of melanoma cell fate by using high-resolution confocal microscopy. We specifically placed the melanoma cells adjacent to premigratory NCCs to study the interactions between the melanoma cells and the NCCs, their ancestral cell type of origin. We find that transplanted human metastatic melanoma cells emerge from the chick neural tube, respond to the local microenvironmental cues to sort into NCC migratory pathways, and target peripheral destinations typical of host NCCs. Importantly, the transplanted metastatic melanoma cells do not form tumors. Rather, individual melanoma cells blend in with developing chick structures and display cell morphologies that resemble host NCCs. When we investigated whether invading melanoma cells exposed to the NCC microenvironment alter their molecular phenotype, we observed that a subpopulation expresses a specific melanocyte marker, MART-1, and a neuronal marker, TuJ1, which they did not express at the time of transplantation.

Human metastatic melanoma cells follow NCC migratory pathways with or without the presence of host NCCs, suggesting that melanoma cells invade the chick periphery in a programmed manner. Forty-eight hours after transplantation into either the midbrain, r1, r4, r6, or the trunk neural tube, melanoma cells migrate into positions that correlate with stereotypical NCC migratory pathways (Figs. 1 and 3). Rather than nonspecifically disseminating from the transplantation sites, melanoma cells migrate to (Fig. 6 *S* and *T* and Movies 1 and 2) and congregate in typical NCC destinations, including the branchial arches (Fig. 1), DRG, and SG (Fig. 3). Extension of the egg re-incubation time to 96 h showed that the transplanted melanoma cells did not form tumors (Fig. 6 *H* and *J*). However, these melanoma cells maintained their tumorigenic phenotype in a mouse model during the approximate time period (Fig. 6*K*). When premigratory host NCCs are ablated and replaced with melanoma cells, the tumor cells continue to reach the peripheral host NCC destinations (Figs. 4 and 6 *A* and *C*), suggesting that a NCC scaffold is not necessary to guide melanoma-cell invasion. Indeed, our data support the observations of Mintz and Illmensee (1) that showed malignant mouse teratocarcinoma cells introduced into an embryonic mouse environment contribute to normal embryonic structures. Invading melanoma cells display cell morphologies similar to host NCCs, including cell–cell connections, long filopodia, and chain-like arrays (Fig. 2). Cell–cell connections have been shown to play a role in chick NCC guidance (26), and, therefore, it will be interesting to pursue the migratory behavior and trajectories of human melanoma cells to determine whether there are any differences when host NCCs are present.

Transplanted melanoma cells avoid stereotypical NCC-free zones, suggesting that melanoma cells respond to guidance cues in the chick embryonic microenvironment. Melanoma cells transplanted directly into r3 fail to invade and populate the region lateral to r3 (Fig. 4 *G–I*); melanoma cells transplanted into the even-numbered rhombomeres, such as r4, form into a migratory stream around the otic vesicle and do not invade the area lateral to r3 (Fig. 4 *E* and *F*); and melanoma cells transplanted into the trunk neural tube avoid migrating through the caudal regions of individual somites (Fig. 3*D*). Whether transplanted melanoma cells receive cues from the neural tube or respond to inhibitory signals in the chick microenvironment is an intriguing question. In a typical vertebrate embryo, it is thought that a combination of intrinsic factors, in the form of signals from the neural tube, and extrinsic signals from the environment and other NCCs sculpt the NCC migration pattern (23). In the absence of further time-lapse data, we could not determine whether transplanted melanoma cells migrated into the regions lateral to r3 or the caudal somite and then changed direction to join neighboring streams in a manner similar to that observed in NCCs (27). Another possibility is that melanoma cells transplanted into r3 received signals that inhibited their emigration from the neural tube, a hypothesis suggested for NCCs that originate from r3 and r5 (24). In either scenario, our results suggest a fertile area to explore chick embryonic microenvironmental cues as a means to control melanoma cell invasion.

The metastatic melanoma cells transplanted into the chick trunk neural tube populate ventral sites of the DRG and SG, suggesting that melanoma cells respond to cues typically followed by NCC precursors adopting a neuronal cell fate. Although transplanted melanoma cells are found along both the dorsolateral and dorsoventral trunk NCC migratory pathways, we observed larger numbers of melanoma cells that populated the ventral sites (Fig. 3 *C–E*). It is interesting that tumor cells populated ventral sites typical of neuronal NCC precursors rather than following dorsolateral migratory pathways thought to be linked to NCCs that become melanocytes (28). There is an ongoing debate in the NCC literature as to when trunk NCCs truly adopt a particular cell fate (29). Cell-lineage studies suggest that trunk NCCs may have some predetermination, such that neuronal and melanogenic precursors are separate in time of emergence and migratory pathway (30–32) or may emerge together, stochastically choosing a migratory pathway and adopting a cell fate near the destination site (33). Whether melanoma cells that follow a dorsoventral route simply follow the initial emerging NCCs to those locations or interpret embryonic cell-guidance cues of neuronal precursors is not known. It will be interesting to investigate whether the melanoma cells that populate the SG begin to express neuronal markers. Further tumor cell transplantation studies that focus on the timing of the transplantation in relation to the emergence of the host trunk NCCs may provide helpful insights into potential guidance cues that inhibit or promote melanoma cell invasion and possible reversion to a particular phenotype.

Our results support the hypothesis that signals in an embryonic chick microenvironment play an important role in human melanoma cell migration and reversion of the metastatic phenotype. We have exploited the relationship between melanoma cells and their ancestral NCC phenotype, within the visually and experimentally accessible intact chick embryo. We show promising results that the chick embryonic microenvironment suppresses the tumorigenic phenotype and reprograms the metastatic phenotype of a subpopulation of tumor cells. Our results have promising implications, suggesting that the chick neural-crest-rich microenvironment inhibits the aggressive dissemination of melanoma cells, possibly by using similar signaling pathways that sculpt NCCs into segregated streams to ensure that cells arrive at specific destinations with the

appropriate phenotype. By using this innovative approach, further investigation of the cellular and molecular interactions within the tumor cell embryonic chick microenvironment should allow us to identify and test potential candidate molecules to control and reprogram the metastatic melanoma phenotype.

Materials and Methods

Chick Embryos. Fertile White Leghorn chick eggs were acquired from a local supplier (Ozark Hatchery, Neosho, MO) and incubated at 38°C until the ≈6- to 8-somite stage of development. Eggs were rinsed with 70% alcohol and 3 ml of albumin removed before cutting a window in the shell. A solution of 10% India ink in Howard Ringer's solution was injected below the blastodisc to visualize the embryos. Embryos were staged according to the criteria of Hamburger and Hamilton (34).

Cell Culture. The adult human metastatic cutaneous melanoma cell line C8161 and its poorly aggressive isogenic counterpart C81-61 were isolated from an abdominal wall metastasis (35) and maintained as described in ref. 9. Normal human melanocytes (HEMn) isolated from neonatal foreskins were maintained in Medium 254 with Human Melanocyte Growth Supplement (Cascade Biologics, Portland, OR) and gentamycin sulfate. All cultures were determined to be free of mycoplasma contamination by using a PCR-based detection system (Roche, Indianapolis).

Western and Immunofluorescence Analyses. C8161 and C81-61 human melanoma cells and HEMn melanocytes were lysed in RIPA buffer plus protease inhibitors (36), sonicated, and centrifuged at 11,300 × *g* for 35 min at 4°C for Western analysis. Fifteen micrograms of protein were then loaded per well of a 4–12% Bis-Tris polyacrylamide gel (Invitrogen) and electroblotted onto an Immobilon-P membrane (Millipore, Bedford, MA), and MART-1 was detected by using an anti-MART-1 antibody (M2410, 1:100, U.S. Biological, Swampscott, MA). Equal loading of protein was demonstrated by using an anti-actin antibody (MAB1501, 1:5,000, Chemicon, Temecula, CA). Neuronal marker and MART-1 expression by immunofluorescence microscopy was evaluated as described in refs. 36 and 37**.** Tissue sections were stained by using the Tuj1 primary antibody (Chemicon) expressed exclusively by neurons (38), P0, a glial marker (from the Developmental Studies Hybridoma Bank, University of Iowa, Iowa City, IA), Hu RNA-binding protein (a gift from J. Weston, University of Oregon, Eugene, Oregon), and MART-1. Anti-GFP antibody (Molecular Probes) was used to detect melanoma cells after fixation (37).

Tumor Cell Transplantations. Small subpopulations of melanoma cells, prepared as tumor cell drops (see *Supporting Materials and Methods*, which is published as supporting information on the PNAS web site, for a description) were cut from appropriate clumps into rectangular blocks ≈100 μm × 50 μm (wide) × 50 μm (thick) by using a sharpened tungsten needle. We estimated that for each transplantable block of melanoma cells, there were ≈1,550 ± 200 individual GFP-labeled cells, determined by adding 50 ml of 0.25% Trypsin (GIBCO) in DMEM to the blocks ($n = 5$). Subpopulations of poorly aggressive C81-61 melanoma cells were prepared for transplantation in the same manner.

Chick embryos (6- to 8-somites) were prepared for transplantation of melanoma cells by cutting a hole in the vitelline membrane above the neural tube by using a sharpened tungsten needle. The melanoma cell block was then guided into the incision by using the glass needle and was gently tucked into the neural tube. For chick embryos in which the host NCCs were ablated before the transplantation of melanoma cells, incisions were made with a glass needle in a specific region of the neural tube. In some host embryos, a lipophilic dye (DiI, Molecular Probes) was injected before ablation to label host NCCs.

Static Imaging. For static imaging, individual embryos were removed from eggs with paper rings, rinsed with Ringer's solution and placed dorsal side up within a thin ring of high-vacuum grease (Dow Corning, Midland, MI) on 22- × 75-mm microslides. Embryos were imaged by using one of two laser scanning confocal microscopes (LSM 510 Meta and LSM 5 Pascal, Zeiss).

Time-Lapse Confocal Imaging. Whole-embryo cultures were prepared and imaged as described in ref. 16. All time-lapse imaging sessions ($n = 6$) used a Plan-Neofluor 10×/0.3 dry objective, optical zoom = 2 and 5-min time intervals, with an inverted confocal microscope (LSM 5 Pascal, Zeiss).

We gratefully acknowledge the research expertise of Dr. Lynne-Marie Postovit (Children's Memorial Research Center). This work was supported by National Institutes of Health/National Cancer Institute Grant CA59702 (to M.J.C.H.) and the Stowers Institute for Medical Research (P.M.K.).

1. Mintz, B. & Illmensee, K. (1975) *Proc. Natl. Acad. Sci. USA* **72,** 3585–3589.
2. Dolberg, D. S. & Bissell, M. J. (1984) *Nature* **309,** 552–556.
3. Erickson, C. A., Tosney, K. W. & Weston, J. A. (1980) *Dev. Biol.* **77,** 142–156.
4. Kenny, P. A. & Bissell, M. J. (2003) *Int. J. Cancer* **107,** 688–695.
5. Hochedlinger, K., Blelloch, R., Brennan, C., Yamada, Y., Kim, M., Chin, L. & Jaenisch, R. (2004) *Genes Dev.* **18,** 1875–1885.
6. Bittner, M., Meltzer, P., Chen, Y., Jiang, Y., Seftor, E., Hendrix, M., Radmacher, M., Simon, R., Yakhini, Z., Ben-Dor, A., *et al.* (2000) *Nature* **406,** 536–540.
7. Hendrix, M. J., Seftor, E. A., Hess, A. R. & Seftor, R. E. (2003) *Nat. Rev. Cancer* **3,** 411–421.
8. Seftor, E. A., Meltzer, P. S., Schatteman, G. C., Gruman, L. M., Hess, A. R., Kirschmann, D. A., Seftor, R. E. & Hendrix, M. J. (2002) *Crit. Rev. Oncol. Hematol.* **44,** 17–27.
9. Hendrix, M. J., Seftor, R. E., Seftor, E. A., Gruman, L. M., Lee, L. M., Nickoloff, B. J., Miele, L., Sheriff, D. D. & Schatteman, G. C. (2002) *Cancer Res.* **62,** 665–668.
10. Lee, L. M., Seftor, E. A., Bonde, G., Cornell, R. A. & Hendrix, M. J. (2005) *Dev. Dyn.* **233,** 1560–1570.
11. Hay, E. D. (2005) *Dev. Dyn.* **233,** 706–720.
12. Le Douarin, N. & Kalcheim, C. (1999) *The Neural Crest* (Cambridge Univ. Press, Cambridge, U.K.).
13. Rickmann, M., Fawcett, J. W. & Keynes, R. J. (1985) *J. Embryol. Exp. Morphol.* **90,** 437–455.
14. Lumsden, A. & Keynes, R. (1989) *Nature* **337,** 424–428.
15. Schilling, T. F. & Kimmel, C. B. (1994) *Development (Cambridge, U.K.)* **120,** 483–494.
16. Kulesa, P. M. & Fraser, S. E. (1998) *Int. J. Dev. Biol.* **42,** 385–392.
17. Farlie, P. G., Kerr, R., Thomas, P., Symes, T., Minichiello, J., Hearn, C. J. & Newgreen, D. (1999) *Dev. Biol.* **213,** 70–84.
18. Sechrist, J., Serbedzija, G. N., Scherson, T., Fraser, S. E. & Bronner-Fraser, M. (1993) *Development (Cambridge, U.K.)* **118,** 691–703.
19. Birgbauer, E., Sechrist, J., Bronner-Fraser, M. & Fraser, S. (1995) *Development (Cambridge, U.K.)* **121,** 935–945.
20. Krull, C. E., Collazo, A., Fraser, S. E. & Bronner-Fraser, M. (1995) *Development (Cambridge, U.K.)* **121,** 3733–3743.
21. Trainor, P. & Krumlauf, R. (2000) *Nat. Cell. Biol.* **2,** 96–102.
22. Kulesa, P., Ellies, D. L. & Trainor, P. A. (2004) *Dev. Dyn.* **229,** 14–29.
23. Krull, C. E. (2001) *Mech. Dev.* **105,** 37–45.
24. Graham, A., Begbie, J. & McGonnell, I. (2004) *Dev. Dyn.* **229,** 5–13.
25. Takeuchi, H., Kuo, C., Morton, D. L., Wang, H. J. & Hoon, D. S. (2003) *Cancer Res.* **63,** 441–448.
26. Teddy, J. M. & Kulesa, P. M. (2004) *Development (Cambridge, U.K.)* **131,** 6141–6151.
27. Kulesa, P. M. & Fraser, S. E. (1998) *Dev. Biol.* **204,** 327–344.
28. Loring, J. F. & Erickson, C. A. (1987) *Dev. Biol.* **121,** 220–236.
29. Erickson, C. A. & Reedy, M. V. (1998) *Curr. Top. Dev. Biol.* **40,** 177–209.
30. Henion, P. D. & Weston, J. A. (1997) *Development (Cambridge, U.K.)* **124,** 4351–4359.
31. Reedy, M. V., Faraco, C. D. & Erickson, C. A. (1998) *Dev. Biol.* **200,** 234–246.
32. Kos, K., Fine, L. & Coulombe, J. N. (2001) *J. Neurobiol.* **47,** 93–108.
33. Bronner-Fraser, M. & Fraser, S. E. (1988) *Nature* **335,** 161–164.
34. Hamburger, V. & Hamilton, H. L. (1951) *J. Morphol.* **88,** 49–92.
35. Welch, D. R., Bisi, J. E., Miller, B. E., Conaway, D., Seftor, E. A., Yohem, K. H., Gilmore, L. B., Seftor, R. E., Nakajima, M. & Hendrix, M. J. (1991) *Int. J. Cancer* **47,** 227–237.
36. Seftor, E. A., Brown, K., Chin, L., Kirschmann, D. A., Wheaton, W. W., Protopopov, A., Feng, B., Balagurunathan, Y., Trent, J., Nickoloff, B. J., *et al.* (2005) *Cancer Res.* **65,** 10164–10169.
37. Rifkin, J. T., Todd, V. J., Anderson, L. W., Lefcort, F. (2000) *Dev. Biol.* **227,** 465–480.
38. Lee, M. K., Tuttle, J. B., Rebhun, L. I., Cleveland, D. W. & Frankfurter, A. (1990) *Cell Motil. Cytoskeleton* **17,** 118–132.